ISSN: 2093-5374 / E-ISSN: 2093-5382

Comparative Analysis of LSTM and BiLSTM in Image Detection Processing

Dr. Bob Subhan Riza[1*], Dr. Rina Yunita[2], and Dr. Rika Rosnelly[3]

[1*]Faculty of Engineering and Computer Science, University of Potensi Utama, Medan, Indonesia.
bob.potensi@gmail.com, https://orcid.org/0000-0001-6358-9412

[2]H Adam Malik Central RSU at the Diagnostic Laboratory Installation for the Clinical Microbiology Sub-unit, Indonesia. rina.yunita@usu.ac.id, https://orcid.org/0000-0001-5426-064X

[3]Faculty of Engineering and Computer Science, University of Potensi Utama, Medan, Indonesia.
rikarosnelly@gmail.com, rika@potensi-utama.ac.id, https://orcid.org/0000-0002-0407-5160

Received: September 28, 2023; Revised: November 30, 2023; Accepted: January 30, 2024; Published: March 30, 2024

Abstract

Tuberculosis is an infectious disease and requires serious treatment. Extrapulmonary Tuberculosis is detected using a microscope. Currently it will take a long time because the fluid preparations are viewed in a microscope one by one carefully and in the fluid preparations there are 150 fields of vision. Examination for Extra Pulmonary Tuberculosis by culture takes between 1-2 weeks or even more. Examination by biopsy will take a long time because the fluid preparations are looked at carefully under the microscope one by one. The image of Tuberculosis is expressed if in the image there is a bacillus object in red, and it turns out that apart from the bacillus object there are other objects also in red. So that examinations for tuberculosis can be more efficient, examinations using computer technology are needed. This research aims to compare the Long Short-Term Memory (LSTM) and Bidirectional Long Short-Term Memory (BiLSTM) classification methods in the detection of extra-pulmonary tuberculosis disease to obtain better accuracy results. This research carried out HSI color space transformation, segmentation using global thresholding, feature extraction using 13 features based on shape and texture using the Correlation Based Feature Selection (CFS) feature selection method. The results show that BiLSTM has the best accuracy with a value of 88.40% at the number of features = 3, namely Short Run High Gray-Level Emphasis, Run Length Nonuniformity, Minor axis length, while LSTM produces an accuracy of 63.19% at the number of features = 5. BiLSTM is capable of detecting opposite features, meaning that BiLSTM can detect opposite features in data sequences and BiLSTM's ability to understand multiple contexts, so it tends to provide more accurate results in some data classification tasks.

Keywords: TBEP Detection, Global Thresholding, CFS, LSTM, BiLSTM.

1 Introduction

The development of Artificial Intelligence (AI) technology is one of the most popular technologies today. Various industrial fields have utilized AI technology, ranging from finance, medical and others. Machines or computers with Artificial Intelligence capabilities can carry out learning based on

Journal of Wireless Mobile Networks, Ubiquitous Computing, and Dependable Applications (JoWUA), volume: 15, number: 1 (March), pp. 244-260. DOI: *10.58346/JOWUA.2024.I1.017*

*Corresponding author: Faculty of Engineering and Computer Science, University of Potensi Utama, Medan, Indonesia.

experience derived from data processing to perform certain tasks. The quality and quantity of tasks processed greatly determines the quality and quantity obtained by the machine or computer. AI is also called artificial intelligence, which is a science that has several branches, one of which is Machine Learning (ML). ML is a computer application and mathematical algorithm that is adopted by learning from data and producing future predictions (Goldberg, D.E., 1988). Currently it is very developed and has been used in various fields, one of which is the health sector. Several studies have developed machine learning and created a new branch, namely Deep Learning.

Deep learning is part of machine learning, applied to Artificial Neural Network (ANN) in 2000. Deep learning is able to teach computers to do work like humans do. Deep learning has hundreds of layers, maybe even more, that's why it is called deep learning. One of the capabilities of Deep learning is being able to replace hand-crafted features with more efficient algorithms for unsupervised hierarchical learning or semi-supervised feature learning and hierarchical feature extraction. The application of deep learning has been used in several fields such as image classification, text to speech, video classification, object detection, natural processing, text classification and robotics (Schmidhuber, J., 2015).

Tuberculosis (TB) is a persistent and contagious illness impacting humans worldwide, necessitating intricate therapies. With around 10 million new instances and 1.3 million fatalities each year, TB remains a critical concern for global health (Rajakumar, M.P., 2021) (World Health Organization (WHO), 2021).

Tuberculosis detection tests obtained using conventional methods such as blood, culture, sputum and biopsy take a long time, i.e. 1-2 weeks or more to give results. (Hasanuddin, A., 2022). Diagnosis of tuberculosis based on bacteriological or clinical factors can be grouped according to the anatomical location. There are two types of lung tubercles and extrapulmonary tubercles. Pulmonary tuberculosis is a case of TB involving the lung parenchym; extrapulmonary TB involves the organs outside the parenchyme of the lung, such as the pleura, lymph gland, abdomen, joints, bones, genitourinary tract, skin, and brain membrane (Triyani, Y., 2020). It will take a while to detect tuberculosis microscopically at this stage because each liquid preparation is examined in detail under a microscope one at a time (Paul, D.C., 2022). The preparations that contain basil tuberculosis and non-tuberculosis have 150 fields of vision when examined under a microscope. Preparations of Tuberculosis and Non-Tuberculosis bacilli, by carrying out the digitization process will produce images of Tuberculosis and Non-Tuberculosis bacilli, then the image data is ready to be processed using image processing and pattern recognition (Venugopal, R.M., 2023).

In order to assess how well deep learning classification techniques, such as long-short-term memory (LSTM) and bi-directional long-short-term memory (BiL STM), detect extrapulmonary tuberculosis illness, a comparison of these techniques was conducted in this work.

The Long Short-Term Memory (LSTM) algorithm is an evolution of the Recurrent Neural Network (RNN) algorithm to overcome RNN problems in managing data for long periods. The LSTM algorithm is an algorithm that is better than other algorithms in managing time series data. LSTM produces more successful processes and faster learning (Hochreiter, S., 1997). At vulnerable times the time is very long compared to the known size with important events. This is one of the main reasons why LSTM has become an alternative to RNNs and Hidden Markov models and other sequence learning methods in various applications (PSugiartawan, 2018).

The Bidirectional Long Short-Term Memory (BiLSTM) algorithm enhances the standard Long Short-Term Memory (LSTM) network by incorporating forward LSTM layers to capture preceding context and backward LSTM layers for analyzing subsequent contexts. This approach utilizes a bidirectional structure that links two hidden layers, moving in opposite directions, to a single output.

Operating on the principles of generative deep learning, this configuration allows neuron layers to simultaneously process information from both past and future states. (Isnain, A.R., 2020).

Research related to the detection of Tuberculosis using deep learning classification, namely (Alsaffar, M., 2021) uses 3 classification methods, namely support vector machine, logistic regression, nearest neighbors in detecting Tuberculosis using digital image processing techniques; (Rasyid, A., 2023) used Convolutional Neural Network (CNN) to classify human lung tuberculosis based on Thorax X-ray images. Pattern recognition research uses CNN (Subramanian, B., 2020) (Swetha, K., 2020) (Griffin, T., 2022) (Ahmad Rafiansyah Fauzan, A.R.F., 2021) (Liu, Z., 2022) (Kale, S.P., 2022) (Devasia, J., 2022) (Patel, S.B., 2022) (Singh, V., 2021) (Dey, S., 2022) (Karki, M., 2022) (Wong, A., 2022). The LSTM and BiLSTM methods are still minimal in detecting extra-pulmonary tuberculosis bacilli using images of tuberculosis bacilli from microscopic examination. Research (Subramanian, B., 2020) (Swetha, K., 2020) (Griffin, T., 2022) (Ahmad Rafiansyah Fauzan, A.R.F., 2021) (Liu, Z., 2022) (Kale, S.P., 2022) (Devasia, J., 2022) (Patel, S.B., 2022) (Singh, V., 2021) (Dey, S., 2022) (Karki, M., 2022) (Wong, A., 2022) used CNN for Tuberculosis detection based on sputum. Research using these two methods of classification can show good accuracy for detecting extra pulmonary tuberculosis and can help clinicians as a medical aid that can detect with much more precision computerized than microscopic.

2 Research Methodology

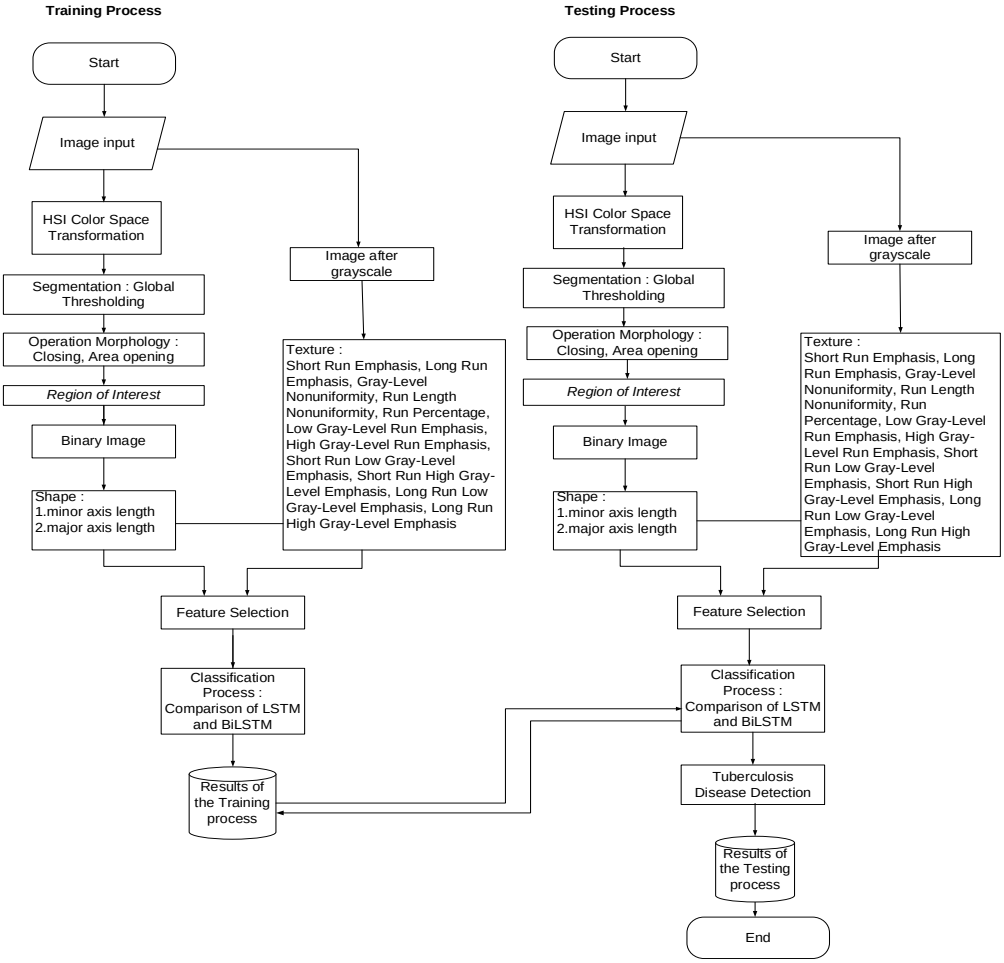

Figure 1: Stages of Research Comparing the Classification of Long Short-term Memory and Bidirectional Long Short-term Memory in the Detection of Extra-pulmonary Tuberculosis Disease

This development uses several image processing techniques and neural networks to carry out detection. In general, the method consists of several parts, namely image acquisition, image transformation, image segmentation, opening, closing, Region of Interest (ROI), feature extraction, feature selection and detection, and each part depends on the results of the previous part. Research stages Comparison of the Classification of Long Short-Term Memory and Bidirectional Long Short-Term Memory in the Detection of Extra Pulmonary Tuberculosis Disease in Figure 1 (Alamer, L., et al., 2023).

a. Image Input
In the process of imaging Extra Pulmonary Tuberculosis (TBEP), a biopsy is performed to extract fluid from an individual. This fluid is then placed onto a slide and stained with Ziehl-Neelsen dye, enhancing visibility under a microscope when observed with immersion oil. These slides are subsequently examined under a digital microscope at 1000x magnification, classifying the findings as either tuberculosis or non-tuberculosis to generate images of TBEP and non-TBEP (Sundhar 2014). The disease images are captured using microscopes that are connected to computers through specific software, simplifying the image acquisition of TBEP. The analysis is conducted using an Olympus BX53 digital microscope, equipped with a 10x ocular lens and a 100x objective lens, achieving a magnification level of 1000x. Illustrations of both TBEP and non-TBEP acid-fast bacilli can be found in Figure 2.

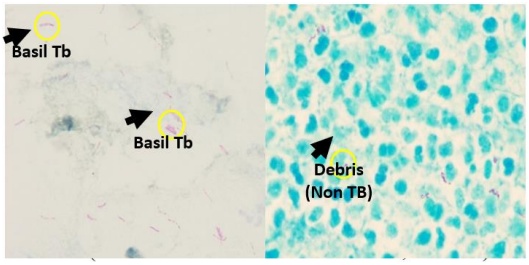

Figure 2: Left: TBEP, Right: Non TBEP

(Source: RSUP. H. Adam Malik, Medan)

Figure 2 shows examples of images captured with a digital microscope such as acid-resistant basil (BTA), extra pulmonary tuberculosis (TBEP) and non-TBEP. In Figure 2, it shows that patients who have extra pulmonary tuberculosis have bacilli (rods) in red and patients who are not affected by tuberculosis have debris, namely residual fuchsin staining, which when seen looks like bacilli (stems) with a red color too. Sampling was done at RSUP by H. Adam Malik Medan. The samples were examined, labeled, and validated by Dr. Rina Yunita, Specialist in Clinical Microbiology, SpMK (K). Given the limitations of the available data, the image captured consisted of 78 images, consisting of 39 TBEP images and 39 non-TBEP pictures, seen using a digital microscope with dimensions of 1920x1440 pixels.

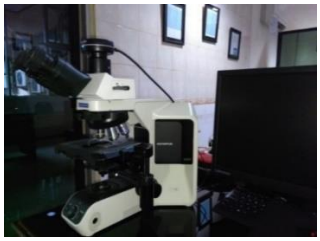

Figure 3: Digital Microscope

(Source: RSUP. H. Adam Malik, Medan)

Figure 3. is an examination tool used to view TBEP and Non-TBEP bacilli. TBEP and Non-TBEP preparations were dripped with immersion oil. Immersion oil is useful for clarifying objects. Next, the preparations are examined using a digital microscope with a magnification of 1000 times, then labeled as TBEP or Non-TBEP, resulting in a TBEP image and a non-TBEP image.

b. Hue, Saturation, Intensity (HSI) Color Space Transformation

Converting image color spaces is a fundamental task in Image Processing, frequently utilized for applying various transformations or filters specific to certain color modes of an image, such as performing thresholding in grayscale or color slicing in HSV. The HSI (Hue, Saturation, Intensity) color space, in particular, has gained significant focus due to its effectiveness in channel analysis for extracting information about images and their components. To facilitate certain operations, converting images into the HSI color space is essential. The process begins by importing an RGB image and normalizing the values of each channel by dividing by 255, resulting in a binary value stored in a variable I. The RGB image's channels are individually extracted and assigned to different variables. Conversion to the HSV color space is achieved through the rgb2hsv function. Subsequently, the Hue and Saturation values are segregated into distinct variables, while the image's intensity level is derived using a specific equation. (Vasu Dev, 2022):

$$\text{Intensity} = (R + G + B)/3 \quad \text{.....} \quad (1)$$

Then a zero matrix is created the same size as the original image, and then filled with Hue, Saturation, and Intensity Channels. Finally, the HSI image is displayed.

c. Segmentation

In the field of biomedical image processing, segmentation plays a crucial role as it enables the separation of physiological and biological structures. Segmentation techniques can generally be categorized into three types: pixel-based, region-based, and edge-detection methods. This particular study aims to segment tissue images into two distinct areas: TBEP and Non-TBEP regions. The TBEP region encompasses elements indicative of TBEP bacilli, whereas the Non-TBEP region includes the image background and other objects. A technique known as thresholding is employed for this segmentation, effectively partitioning the image into object and background regions. In this process, the area representing the object is marked in white, and the remaining area is marked in black, or the inverse. This thresholding results in a binary image displaying only two levels of gray: black and white. The implementation of this technique involves the application of a specific threshold function, denoted as equation 2:

$$T = T[a, b, p(a, b), f(a, b)] \quad (2)$$

where p(a,b) is the pixel value of a certain point and f(a,b) is the pixel intensity (a,b). Next, the image with the threshold will be divided into two parts, as shown in equation 3:

$$g(a, b) = \begin{cases} 1, jika\ f(a, b) > T \\ 0, jika\ f(a, b) \leq T \end{cases} \quad (3)$$

Pixels with a value of 1 indicate objects, while pixels with a value of 0 represent the image background. Global thresholding is the position where T depends on f(a, b) (Gonzales, R.C., 2018). Global thresholding is capable of producing optimum thresholds to distinguish between tuberculosis and non-tuberculosis basil objects.

d. Morphological Operations: Closing and opening areas

Based on the TBEP image that has been obtained and after analysis it can be seen, it turns out that there are several image objects that are small in size, so that after segmentation there are missing pixels, then a closing operation is carried out, where the closing method is to widen the object by carrying out a dilation operation which is then carried out smoothing the edges of objects, namely by erosion operations. Because the shape of the TBEP bacillus tends to be elongated, the structural elements are square in shape. In this

research, a morphological opening operation was carried out to remove small objects that were not bacilli so that the image could smooth the boundaries of the bacilli objects. The closing operation is a dilation operation by structuring element Q, which is followed by successive erosion operations with the same structuring element. Closing the set P by structural element Q. The result of this operation is the closing of gaps or holes that are smaller than the structural elements. Mathematically, the closing operation can be written in equation 4 (Kumar, A., 2022).

$$P \cdot Q = (P \oplus Q) \ominus Q \quad (4)$$

Figure 4 shows the operation closing P by Q, followed by erosion of the result by Q.

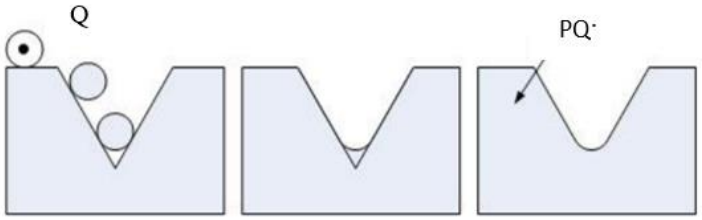

Figure 4: Closing Operation of Image P by Q

In research conducted using a global thresholding algorithm for the segmentation process.

The opening operation is an erosion operation then followed by a dilation operation. Opening smoothes the outlines of objects, eliminates narrow parts and eliminates thin protrusions. The equation of the opening morphology operation can be seen in equation 5.

$$P \cdot Q = (P \ominus Q) \oplus Q \quad (5)$$

Figure 5 shows the operation of opening P by Q, followed by dilation of the result by Q.

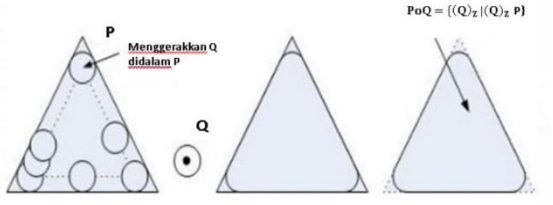

Figure 5: Operation of Opening Image P by Q

e. Region of Interest (ROI)
At this stage, the process of taking the closing and opening images is carried out by cropping using tools in the Matlab programming language to obtain the resulting TBEP image object. Next, the results of the ROI process are resized to a size of 512x512 pixels. The ROI results will be saved in the form of a binary image that is ready to be processed to the feature extraction stage.

f. Feature Extraction
Feature extraction is a process to extract an image into a value so that based on this value it can differentiate between acid-fast bacilli (BTA) objects or what are called TBEP and Non-TBEP. Shape and texture features are a priority because they require better detection of tuberculosis. The shape feature is the main thing because the object of tuberculosis bacilli is different in size from non-tuberculosis. Texture features are a process for extracting an image into a value based on the level of roughness, regularity, and irregularity so that, based on this value, it can differentiate between tuberculosis and non-tuberculosis bacilli objects. This research with hyper features uses shape and texture features, namely minor axis length, major axis length, Short Run Emphasis, Short Run Low Gray-Level Emphasis, Short Run High Gray-Level Emphasis, Long Run Emphasis, Low Gray-Level

Run Emphasis, Long Run Low Gray-Level Emphasis, Long Run High Gray-Level Emphasis, Run Percentage, Run Length Nonuniformity, Gray-Level Nonuniformity, High Gray-Level Run Emphasis.

g. Feature Selection
Feature selection is a preprocessing stage for detection. This research uses Correlation Based Feature Selection for the feature selection stage, where Correlation Based Feature Selection is an attribute selection technique in a dataset which is carried out by calculating the relationship between predicted attributes and target attributes, where the selected attributes are attributes that have a high correlation between predicted attributes and attributes. targets, but have low association values with other attributes and high linear relationships with labels resulting in better performance in terms of accuracy (Yayik., A., 2017).

h. Classification
The classification stage will compare two Deep Learning methods, namely Long Short-Term Memory (LSTM) and Bidirectional Long Short-Term Memory (BiLSTM). The main advantage of LSTM is:

1. Understand the long sequence. Its ability to deal with the problem of gradual loss that often occurs in RNNs
2. Long-term and short-term memory LSTM has two types of internal memory, namely long-term memory and short-term memory. Long-term memory allows LSTS to store relevant information from the past, while short-term memory allows models to store more recent information. This helps LSTMS identify important contexts in the data sequence.
3. Flexibility. LSTM is a flexible and variable architecture for a wide range of tasks; it can adjust the number of layers, the number of units in each layer, and configure various parameters to optimize model performance.

Advantages of BiLSTM:

1. Double-context understanding BiLSTM is a variant of the LSTM that has two layers that work together, one processing data from the beginning to the end of a sequence (forward L STM) and the other from the end to the beginning (backward L STM). This allows the BiL STM to understand the context of both directions in a data sequence. This is very useful in tasks where the context is in two directions.
2. detection of opposite features BiLSTM can detect opposing features in a data sequence.
3. Better accuracy Due to its ability to understand multiple contexts, BiLSTM tends to deliver more accurate results in several data classification tasks compared to a single LSTM.

LSTM and BiLSTM were applied to 78 images consisting of 39 TBEP images and 39 Non-TBEP images with 70 training data consisting of TBEP and Non-TBEP object data.

- Long Short-Term Memory (LSTM)
LSTM, or Long Short-Term Memory, is a type of neural network that boasts a flexible architecture, allowing its shape to be tailored to suit various applications. It is evolved from the Recurrent Neural Network (RNN) technique, which is expressly crafted for processing sequential data. However, RNNs are prone to issues of vanishing and exploding gradients, characterized by significant shifts in the value range from one layer to the next within the network's architecture. The LSTM architecture is designed to overcome these challenges. The application of LSTM in detecting extra pulmonary tuberculosis is depicted in Figure 6.

Figure 6: Long Short-Term Memory (LSTM) Architecture

Figure 6 illustrates the fundamental elements of an LSTM neural network, highlighting the sequence input layer and the LSTM layer as its core components. The sequence input layer is designed to input sequence or time series data into the network. Meanwhile, the LSTM layer is adept at learning the long-term dependencies present between the time steps in sequence data. The figure depicts a straightforward LSTM neural network setup aimed at classification tasks. The network architecture begins with a sequence input layer, followed by an LSTM layer. For the purpose of predicting class labels, the architecture concludes with a fully connected layer, a softmax layer, and a classification layer, which collectively facilitate the identification of Tuberculosis or non-Tuberculosis.

- Bidirectional Long Short-Term Memory (BiLSTM)
  RNNs have demonstrated effectiveness in various acoustic classification endeavors, where acoustic feature vectors are analyzed in a sequence, each influencing the network's internal hidden state. This state, rich in contextual information, evolves with each timestep, enabling the network to capture temporal correlations crucial for the specific classification task. In our research, we adopt the BiLSTM model, an advancement of the LSTM framework, which analyzes sequence data in both forward and backward temporal directions. A notable limitation of traditional LSTM models is their inadequate consideration of information from the final elements in a sequence, as they process data in a singular, start-to-finish direction. To address this, the bidirectional LSTM (BiLSTM) approach processes data bidirectionally, from start to end and end to start, effectively employing two distinct LSTMs for each direction. The forward and backward hidden states, *h*s forward and *h*s backward, are integrated into a comprehensive final hidden state *h*s BiLSTM, as illustrated in equation 6. This bidirectional architecture is depicted in Figure 7, showcasing how BiLSTM enhances data interpretation from both directions (Hochreiter, S., 1997) (Elfaik, H., 2020).

$$hs^{BiLSTM} = hs^{forward} \oplus hs^{backward} \quad (6)$$

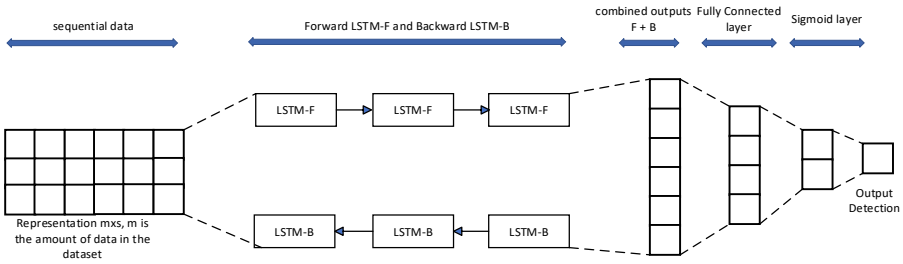

Figure 7: BiLSTM Architecture Implemented

i. Detection Results
At this stage it is useful to find out the results of detecting TBEP or Non-TBEP disease. With 78 TBEP and Non-TBEP image data, after carrying out the training and testing process, TBEP or Non-TBEP detection results were obtained by producing accuracy values. Equation 7 is the accuracy equation (Deeks, J.J., 2023):

$$Akurasi = \frac{TP+TN}{TP+TN+FP+FN} \quad (7)$$

with,
T.P: the number declared positive by the test and optimal by the gold standard.
F.P: the number declared positive by the test and the gold standard says it is not optimal.
FN: the amount declared negative by the test and optimal by the gold standard.
TN: amount declared negative by the test and not optimal by the gold standard.

3 Results and Discussion

The model designed based on the research methodology is then the result of the methodology and includes a discussion at each stage.

3.1 Image Input

Figure 8 shows TBEP and non-TBEP images. In the TBEP image, the characteristics are that it is a slender and thin rod, can be straight or bent and has a red color that is acid-resistant. They are called acid-fast bacilli (BTA) because they are difficult to decolorize with alcohol or acid. In the Non-TBEP image, there is debris, which is the crystallization of dissolved cations in the washing water originating from the laboratory water source in the form of elongated red lumps.

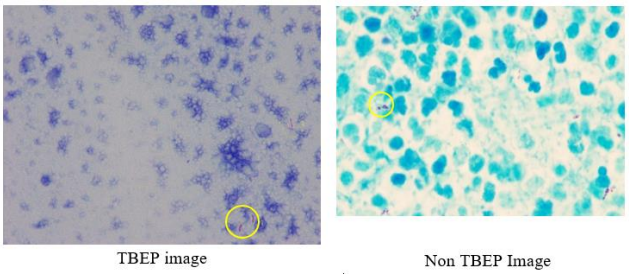

Figure 8: Image TBEP and Non TBEP

3.2 HSI Color Space Transformation Results

After taking the TBEP and Non-TBEP images, the next step is to carry out the HSI color space transformation. The color space transformation process is carried out to obtain HSI color space image results. In this stage, the H component will be taken because the H component is not affected by the uneven light intensity in the image of tuberculosis bacilli and non-bacilli. The input for this stage is in the form of images of Tuberculosis bacilli and non-bacilli. The HSI color space looks more realistic in describing colors naturally and intuitively for humans, so it can be said that HSI is very suitable for describing colors while RGB is suitable for producing colors. Hue is the angle between the reference color and the Saturation vector. The reference color is usually red but can be other colors. The H value is between 00-3600 on the red axis. This angle depicts pure colors diluted by white light. The H value is said to be the dominant color of the image. The S value is the length of the distance from the origin point (the center of mass of the plane) to an arbitrary point where the arbitrary point is a color point. The intensity of the color is indicated by the position of the plane on the vertical axis. The higher the position of the field on the vertical axis of intensity, the greater the I value and vice versa. One example of the results of a Tuberculosis image in RGB color space into HSI can be seen in Figure 9.

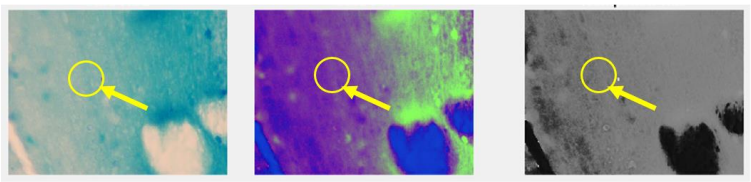

Figure 9: (a) Image of Tuberculosis Bacilli in RGB Color (b) Image Results of Tuberculosis Bacilli in HSI Color (c) Results of Images of Tuberculosis Bacilli in Hue Component

Figure 9. is the result of the HSI color space transformation, namely the Hue component, where it can be seen that it has differentiated between the object and the background? The image extracted from the Hue component will be saved and used for the segmentation stage.

3.3 Segmentation Results

The segmentation phase is critical for isolating the desired object from its background. During this process, acid-fast bacilli (AFB) are distinguished from other elements, including debris and necrotic cells. This begins with retrieving image data from the Hue component and applying Global Thresholding. Global Thresholding is chosen for its effectiveness in establishing an optimal threshold in this study, facilitating the distinction between TBEP and non-TBEP objects within the foreground from the background. This segmentation step employing global thresholding is depicted in Figure 10.

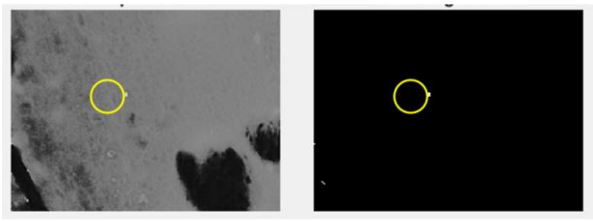

Figure 10: (a) Tuberculosis Bacillus Image Results with Hue Component (b) Image Segmentation Results using Global Thresholding

Figure 10. (a) is the result of the Hue component. Figure 10 (b) is the result of segmentation using global thresholding. The advantage of using global thresholding is that there is no need to set the threshold value manually. and in this research, we can separate BTA objects from the background.

3.4 Results of Morphological Operations: Closing and Opening Areas

The outcomes of the morphological analysis, employing closing and opening techniques, are illustrated in Figure 11. These morphological operations are designed to modify the object's form in the initial image by eliminating surrounding elements of the acid-fast bacilli (AFB). Figure 11 showcases an instance of the morphological analysis outcomes for the TBEP positive category, as seen from Figure 11(a).

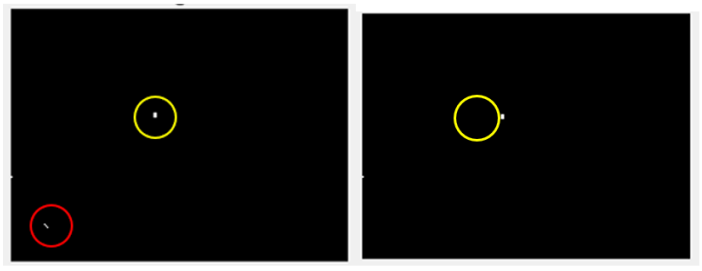

Figure 11: (a) Image from Global Thresholding Segmentation Results (b) Example of Closing and Opening Operation Results

The image resulting from the segmentation process is then processed to the morphological analysis stage. In Figure 11 (a) and (b) you can see the difference, where in Figure 11 (a), the result of the TBEP image using global thresholding, there is still noise in the form of other objects, namely small white

spots (in the red circle), so noise removal is carried out using morphology. closing and opening mathematics. Figure 11 (b) After carrying out the closing and opening mathematical morphology, the noise is no longer visible.

Next, cropping is carried out automatically, which is the delimiter of the TBEP and Non-TBEP objects, where 78 TBEP and Non-TBEP image data are cut.

3.5 Region of Interest (ROI) Results

Based on the TBEP image resulting from morphological operations that have gone through a noise removal process, we proceed to the region of interest process, namely cropping the image of the TBEP result. The TBEP bacillus image is taken for use in the next process. The cropped image of the TBEP bacillus can be seen in Figure 12.

(a) (b)

Figure 12: (a) Results of Morphological Analysis of the TBEP Class (b) Cropping Results

Figure 12 (a) is an example of an image resulting from morphological analysis of TBEP bacilli using closing and opening, and Figure 12 (b) is an image of cropping TBEP bacilli. The cropped image is then used in the extraction stage.

3.6 Feature Extraction Results

After being processed for Region of Interest (ROI), the TBEP bacillus image undergoes cropping, followed by feature extraction to identify its predominant characteristics. The texture analysis leverages the Gray Level Co-Occurrence Matrix (GLCM), which assesses the likelihood of adjacent pixel relationships at a specific distance, with the choice of distance being a crucial factor in GLCM analysis. This study opts for a spatial distance of 1 for its simplicity in computation. Feature extraction from the TBEP image incorporates a variety of metrics, including minor and major axis lengths, along with a series of emphasis metrics such as Short Run Emphasis, Short Run Low Gray-Level Emphasis, Short Run High Gray-Level Emphasis, Long Run Emphasis, Low Gray-Level Run Emphasis, Long Run Low Gray-Level Emphasis, Long Run High Gray-Level Emphasis, Run Percentage, Run Length Nonuniformity, Gray-Level Nonuniformity, and High Gray-Level Run Emphasis. Table 1 presents an example of the feature values derived from the extraction process, showcasing the outcomes for both TBEP and Non-TBEP images based on 12 distinct features.

Table 1: Example of Feature Value Results with 12 Features

5.6133	11.7215	0.0061	0.2339	1.2237e+03	4.0013	33.6336	0.1820	2.4279	10.1461	0.9640	34.2842
29.0035	6.9282	0.0173	0.5000	215.8204	6.5884	40.9829	0.6900	2.3094	5.6455	0.1353	5.3356
18.0125	6.6804	0.0168	0.4565	287.8866	6.8609	32.6856	0.5435	2.4842	8.9131	0.2629	8.5979
19.1630	12.4130	0.0217	0.5875	182.4672	15.2247	29.4662	0.6227	2.3790	17.5893	0.2580	6.7761
18.5230	12.1861	0.0284	0.7933	126.3221	14.1771	27.1210	0.6954	2.7021	10.3956	0.1502	4.2135
15.0165	13.3304	0.0163	0.6644	318.3834	9.3083	32.1452	0.4764	3.1808	14.1814	0.2756	9.2754
4.9078	7.7745	0.0038	0.1882	1038	4.2500	36	0.1363	2.5110	9.2500	0.8009	28.8333
16.8149	8.3310	0.0278	0.6372	102.7077	14.6261	24.5993	0.6577	5.1705	13.1734	0.2053	4.4591
13.1744	10.2452	0.0157	0.4454	326.5177	7.4957	31.5085	0.4401	2.8322	13.2806	0.2948	9.6946
7.6332	11.4896	0.0076	0.3288	708.4636	3.6836	29.6354	0.2368	3.3612	11.2810	0.9712	25.9438
17.9786	9.9183	0.0169	0.6229	299.7682	6.6596	30.2178	0.5448	2.2971	8.0382	0.4282	11.2320

Table 1 shows examples of feature value results using 12 features, namely in column 1 to column 12:minor axis length, major axis length, Short Run Emphasis, Short Run Low Grey-Level Emphasis, Short Run High Grey-Level Emphasis, Long Run Emphasis, Low Gray-Level Run Emphasis, Long Run Low Grey-Level Emphasis, Long Run High Gray-Level Emphasis, Run Percentage, Run Length Nonuniformity, Gray-Level Nonuniformity, the number of TBEP and non-TBEP images is 78 images with 40 training data images and 38 test data images. Example results are obtained in Table 1. On 40 training data images using 12 features, 42 data objects were produced, found in rows 1 to row 42.

3.7 Feature Selection Results –Correlation-based Feature Selection

Feature selection plays a crucial role in enhancing the accuracy of TBEP detection outcomes, with its primary goal being to expedite the training phase. In this context, Correlation-based Feature Selection (CFS) is employed. CFS operates on a correlation matrix to identify features that have a high correlation within a given class while ensuring these features remain uncorrelated with others. This methodology is based on the Pearson correlation coefficient. From the feature selection process, 13 dominant features were identified. The outcomes of the feature selection using CFS are documented in Table 2.

Table 2: Feature Selection Results Using CFS

No	Feature	Mark
1	Minor axis length	0.4412
2	Major axis length	0.2405
3	Short Run Emphasis	0.0215
4	Short Run Low Grey-Level Emphasis	0.3969
5	Short Run High Gray-Level Emphasis	0.5679
6	Long Run Emphasis	0.2833
7	Low Gray-Level Run Emphasis	0.4347
8	High Grey-Level Run Emphasis	0.4153
9	Long Run Low Grey-Level Emphasis	0.0176
10	Long Run High Gray-Level Emphasis	0.2853
11	Run Percentage	0.0326
12	Run Length Nonuniformity	0.5031
13	Gray-Level Nonuniformity	0.0190

Table 2 shows the correlation search results showing that the Long Run Low Gray-Level Emphasis= feature0.0176has the lowest correlation value, while the highest feature is Short Run High Gray-Level Emphasis=0.5679.

3.8 Detection Results

Detection Results Using Long Short-Term Memory (LSTM)

The TBEP and non-TBEP disease detection stage consists of two processes, namely training and testing. The training stage uses the results of the feature selection process. Training for Tuberculosis detection uses LSTM with 40 image data with details: 20 TBEP image data and 20 non-TBEP image data. Training on the LSTM network is determined by the parameters batch size=40, epoch=100, number neurons in the hidden layer = 100, with the highest number of features = 3,4,5,6,7 features. The training results can be seen in Table 3.

Table 3: Training Results using LSTM

Accuracy Number of features = 3 (%)	Accuracy Number of features = 4 (%)	Accuracy Number of features = 5 (%)	Accuracy Number of features = 6 (%)	Accuracy Number of features = 7 (%)
90.48%	90.48%	90.48%	88.09%	85.71%

Table 3 shows the accuracy results for TBEP and non-TBEP detection using LSTM. This research was carried out with 3,4,5,6,7 highest features based on correlation values using CFS. The results show that in the training process the highest accuracy is at the number of features = 3,4,5with an accuracy value of 90.48%. The test results can be seen in Table 4.

Table 4: Test Results using LSTM

Accuracy Number of features = 3 (%)	Accuracy Number of features = 4 (%)	Accuracy Number of features = 5 (%)	Accuracy Number of features = 6 (%)	Accuracy Number of features = 7 (%)
59.42%	59.42%	63.19%	61.74 %	62.03 %

The test results in table 4 can be seen using the highest 3,4,5,6,7 features based on the correlation value using CFS, the highest accuracy results at the number of features = 5, namelyShort Run High Gray-Level Emphasis, Run Length Nonuniformity, Minor axis length, Low Gray-Level Run Emphasis, High Gray-Level Run Emphasis. It can be seen that the 5 features with the highest correlation values can influence the accuracy value with a value of 63.19% compared to the number of features 3,4,6,7.

Detection Results using Bidirectional Long Short-Term Memory (BiLSTM)

The training stage for Tuberculosis detection uses BiLSTM with 40 image data with details: 20 TBEP image data and 20 non-TBEP image data. Training on the BiLSTM network uses parameters batch size=40, epoch=100, number neurons in the hidden layer = 100, with the highest number of features = 3,4,5,6,7 features. The training results can be seen in Table 5.

Table 5: Training Results using BiLSTM

Number of features = 3 (%)	Accuracy Number of features = 4 (%)	Accuracy Number of features = 5 (%)	Accuracy Number of features = 6 (%)	Accuracy Number of features = 7 (%)
95.24 %	100%	97.62%	100%	100%

Table 5 shows the accuracy results for TBEP and non-TBEP detection using BiLSTM. This research was carried out with 3,4,5,6,7 highest features based on correlation values using CFS. The results show that in the training process the highest accuracy is at the number of features = 4,6,7,with an accuracy value of 100%. The test results can be seen in Table 6.

Table 6: Test Results using BiLSTM

Accuracy Number of features = 3 (%)	Accuracy Number of features = 4 (%)	Accuracy Number of features = 5 (%)	Accuracy Number of features = 6 (%)	Accuracy Number of features = 7 (%)
88.40 %	86.96 %	87.83 %	73.04 %	72.75 %

Test results in table 6. using 3,4,5,6,7 highest features based on correlation values using CFS, the highest accuracy results at number of features = 3, namely Short Run High Gray-Level Emphasis, Run Length Nonuniformity, Minor axis length. It can be seen that the 3 features with the highest correlation values can influence the accuracy value with a value of 88.40% compared to the number of features 4,5,6,7. The training and testing process with two classification methods and parameters used for TBEP and non-TBEP detection can be seen in Table 7.

Table 7: Results of Accuracy Values at the Training and Testing Stages using the LSTM and BiLSTM Methods

No	Epoch	Amount neurons in the hidden layer	Batch Size	Classification Methods	Training Results (%)	Test result (%)
1	100	100	40	LSTM	90.48	63.19
2	100	100	40	BiLSTM	100	88.40

The results of the comparison of the two classification methods used in table 7 show that the BiLSTM classification method is better with accuracy for testing at 88.40%, while LSTM gets an accuracy of 63.19% because the BiLSTM method is a combination of two LSTMs, namely forward input and backward input. so, when processing input data, it is processed from front to back and from back to front.

4 Conclusion

Based on the results of classification testing for the detection of EPTB and non-EPTB diseases using LSTM and BiLSTM, it can be concluded as follows:

1. The results of training with LSTM produced the best accuracy at the number of features = 3,4,5 with a value of 90.48%, then BiLSTM produced the best accuracy at the number of features = 4,6,7 with a value of 100%.
2. Test results using LSTM using 3,4,5,6,7 features produce the highest accuracy in number of features=5, ie Short Run High Gray-Level Emphasis, Run Length Nonuniformity, Minor axis length, Low Gray-Level Run Emphasis, High Gray-Level Run Emphasis with an accuracy value of 63.19%, then with BiLSTM using the number of features 3,4,5,67 feature produces 88.40% accuracy at number of features = 3, namely Short Run High Gray-Level Emphasis, Run Length Nonuniformity, Minor axis length.
3. The results of this research can be seen that the BiLSTM method produces the best accuracy values, where BiLSTM has dual context understanding, meaning that BiLSTM is a variant of LSTM which has two LSTM layers that work together, one processes data from the beginning to the end of the sequence (forward LSTM), and the other from end to beginning (backward LSTM). This allows BiLSTM to understand context from both directions in the data sequence.

References

[1] Ahmad Rafiansyah Fauzan, A.R.F., Mohammad Iwan Wahyuddin, M.I.W., & Sari Ningsih, S.N. (2021). Pleural effusion classification based on chest x-ray images using convolutional neural network. *Jurnal Ilmu Komputer dan Informasi*, *14*(1), 9-15.

[2] Alsaffar, M., Alshammari, G., Alshammari, A., Aljaloud, S., Almurayziq, T.S., Hamad, A.A., & Belay, A. (2021). Detection of tuberculosis disease using image processing technique. *Mobile Information Systems*, 1-7.

[3] Alamer, L., Alqahtani, I.M., & Shadadi, E. (2023). Intelligent Health Risk and Disease Prediction Using Optimized Naive Bayes Classifier. *Journal of Internet Services and Information Security, 13*(1), 01-10.

[4] Deeks, J.J., Bossuyt, P.M., Leeflang, M.M., & Takwoingi, Y. (Eds.). (2023). *Cochrane handbook for systematic reviews of diagnostic test accuracy*. John Wiley & Sons.

[5] Devasia, J., Goswami, H., Lakshminarayanan, S., Rajaram, M., Adithan, S., & Bharanidharan, A. (2022). Deep Learning Classification of Active Tuberculosis Using Chest X-Rays: Efficacy of Transfer Learning and Generalization Performance of Cross-Population Datasets, 1-12. https://doi.org/10.21203/rs.3.rs-1235165/v1

[6] Dey, S., Roychoudhury, R., Malakar, S., & Sarkar, R. (2022). An optimized fuzzy ensemble of convolutional neural networks for detecting tuberculosis from Chest X-ray images. *Applied Soft Computing*, *114*.

[7] Elfaik, H., & Nfaoui, E.H. (2020). Deep bidirectional LSTM network learning-based sentiment analysis for Arabic text. *Journal of Intelligent Systems*, *30*(1), 395-412.

[8] Goldberg, D.E., & Holland, J.H. (1988). Genetic algorithms and machine learning. *Machine Learning, 3*(2), 95–99.

[9] Gonzales, R.C., Woods, R.E. (2018). Digital Image Processing – Third Edition. New Jersey: Prentice Hall.

[10] Griffin, T., Chen, Q., Sun, X., Wang, D., Brunette, M.J., Cao, Y., & Liu, B. (2022). erxnet: A pipeline of convolutional neural networks for tuberculosis screening. *International Journal of Semantic Computing*, *16*(01), 69-92.

[11] Hasanuddin, A., & Artha, D.E. (2022). The Identification of Mycobacterium Tuberculosis in Active Smokers with Ziehl–Neelsen Staining Method. *International Journal of Public Health Excellence (IJPHE)*, *2*(1), 266-272.

[12] Hochreiter, S., & Schmidhuber, J. (1997). Long short-term memory. *Neural computation*, *9*(8), 1735-1780.

[13] Isnain, A.R., Sihabuddin, A., & Suyanto, Y. (2020). Bidirectional long short-term memory method and Word2vec extraction approach for hate speech detection. *IJCCS (Indonesian Journal of Computing and Cybernetics Systems)*, *14*(2), 169-178.

[14] Kale, S.P., Patil, J., Kshirsagar, A., & Bendre, V. (2022). Early lungs tuberculosis detection using deep learning. In *Intelligent Sustainable Systems: Selected Papers of WorldS4 2021, 1*, 287-294. Springer Singapore.

[15] Karki, M., Kantipudi, K., Yang, F., Yu, H., Wang, Y.X.J., Yaniv, Z., & Jaeger, S. (2022). Generalization challenges in drug-resistant tuberculosis detection from chest X-rays. *Diagnostics*, *12*(1), 1-23.

[16] Kumar, A., Chakravarty, S., Gupta, M., Baig, I., & Albreem, M.A. (2022). Implementation of mathematical morphology technique in binary and grayscale image. *In Advance Concepts of Image Processing and Pattern Recognition: Effective Solution for Global Challenges*, 203-212. Singapore: Springer Singapore.

[17] Liu, Z., Dong, A., Yu, J., Han, Y., Zhou, Y., & Zhao, K. (2022). Scene classification for remote sensing images with self-attention augmented CNN. *IET Image Processing*, *16*(11), 3085-3096.

[18] Patel, S.B., Patel, P.H., Jain, V.D., & Verma, J.P. (2022). Improvised VGG16 CNN Architecture for Predicting Tuberculosis Using the Frontal Chest X-Ray Images. In *Smart Systems: Innovations in Computing: Proceedings of SSIC 2021*, 69-80. Springer Singapore.

[19] Paul, D.C., Ngeow, Y.F., Yap, S.F., Dony, J.F., Avoi, R., Mohammad, R., & Ng, H.F. (2022). Concentrated specimen smear microscopy utilising a polymer membrane sandwich filtration vessel for the detection of acid-fast bacilli in health facilities in Sabah, East Malaysia. *Tuberculosis*, *133*.

[20] Sugiartawan, P., Jiwa Permana, A.A., & Prakoso, P.I. (2018). Forecasting Tourist Visits Using Long Short-Term Memory (LSTM). *J. Sist. Inf. and Comput. Apply. Indonesia., 1*(1), 43–52.

[21] Rajakumar, M.P., Sonia, R., Uma Maheswari, B., & Karuppiah, S.P. (2021). Tuberculosis detection in chest X-ray using Mayfly-algorithm optimized dual-deep-learning features. *Journal of X-Ray Science and Technology*, *29*(6), 961-974.
[22] Rasyid, A., & Heryawan, L. (2023). Classification of Human Lung Organ Tuberculosis (TB) Based on Thorax X-ray Images Using the Convolutional Neural Network (CNN) Method. *Indonesian Journal of Health Information Management*, *11* (1), 35-44.
[23] Schmidhuber, J. (2015). Deep learning in neural networks: An overview. *Neural networks*, *61*, 85-117.
[24] Singh, V., Gourisaria, M.K., Harshvardhan, G.M., & Singh, V. (2021). Mycobacterium tuberculosis detection using CNN ranking approach. In *Advanced Computational Paradigms and Hybrid Intelligent Computing: Proceedings of ICACCP,* 583-596.
[25] Subramanian, B., Harinikaa, M.M., Kritthika, S., Hari Sankar, N. (2020). A Study on Detection of Tuberculosis from Chest X Ray Images and Microscopic Images Based on Deep Learning Techniques. *International Journal of Scientific & Technology Research, 9*(2), 5186-5188.
[26] Sundhar, C., & Archana, D. (2014). Automatic screening of fundus images for detection of diabetic retinopathy. *International Journal of Communication and Computer Technologies (IJCCTS), 2*(1), 29-35.
[27] Swetha, K., Sankaragomathi, B., & Thangamalar, J.B. (2020). Convolutional neural network based automated detection of mycobacterium bacillus from sputum images. *In International Conference on Inventive Computation Technologies (ICICT)*, 293-300.
[28] Triyani, Y., Tejasari, M., Purbaningsih, W., Masria, S., & Respati, T. (2020). The relation of acid fast bacilli with Ziehl Neelsen staining and histopathologic examination of biopsy specimens in extrapulmonary TB suspected patients. *GMHC*, *8*(2), 132-139.
[29] VasuDev4, 2022, How to Convert RGB Image to HSI Image in MATLAB?, MATLAB image-processing, https://www.geeksforgeeks.org/how-to-converting-rgb-image-to-hsi-image-in-matlab/, Access date : June 23, 2023.
[30] Venugopal, R.M. (2023). Efficient Hybrid CNN Method to Classify the Liver Diseases. *Journal of Wireless Mobile Networks, Ubiquitous Computing, and Dependable Applications, 14*(3), 36-47.
[31] Wong, A., Lee, J.R.H., Rahmat-Khah, H., Sabri, A., Alaref, A., & Liu, H. (2022). TB-Net: a tailored, self-attention deep convolutional neural network design for detection of tuberculosis cases from chest X-ray images. *Frontiers in Artificial Intelligence*, *5*, 1-10.
[32] World Health Organization (WHO). Global Tuberculosis Report 2021. Geneva, WHO, 2021. apps.who.int/iris/ bitstream/handle/10665/336069/9789240013131-eng.pdf/ Date last accessed: 19 September 2021
[33] Yayik, A. (2017). Correlation-based feature selection. https://github.com/apdullahyayik/Feature-Selection, access date June 20, 2023.

Authors Biography

Dr. Bob Subhan Riza, ST, M.Kom was born in Medan, North Sumatra on August 5, 1970. As for my Educational History, - D3 at USU Medan Polytechnic graduated in 1993 - S1 at the University of N orth Sumatra, Medan graduated in 2000 - S2 at Putera Indonesia University YPTK Padang graduated in 2014. S3 Information Technology at Putera Indonesia University YPTK Padang graduated in 2023. Currently I am serving as a Permanent Lecturer at Universitas Potensi Utama. My research study in the field of Image Processing.

Dr. Rina Yunita, SpMK (K) is ASN at the Ministry of Higher Education (FK USU). I practices at the H. Adam Malik Central RSU at the Diagnostic Laboratory Installation for the Clinical Microbiology sub-unit.

Dr. Rika Rosnelly, S.Kom, M.Kom was born in Medan, North Sumatra on September 19, 1975. As for my Educational History, S1 at the STMIK Logika Medan graduated in 2005. S2 at Putera Indonesia University YPTK Padang graduated in 2008. S3 Computer Science, at Gadjah Mada University Yogyakarta graduated in 2017. Currently I am serving as a Permanent Lecturer at Universitas Potensi Utama. My research study in the field of Image Processing, Artificial Intelligence, Decision Support System.